Electronic Supplementary Material (ESI) for Journal of Materials Chemistry C.

Electronic Supporting Information (*ESI*)

Silk Fibroin-Carbon Nanoparticle composite Scaffolds: A Cost Effective Supramolecular 'Turn Off' Chemiresistor for Nitro aromatic Explosive Vapours

Sudesna Chakravarty[1#], Nandana Bhardwaj[2#], Biman B. Mandal[3] and Neelotpal Sen Sarma[1]**

1. EDAX Analysis

   The increase is deposition of CNPs in SFC arises due to the availability of large surface area arising out of highly macroporous silk scaffolds. The EDAX profiles of SF and SFC are given below (**Fig. S1**).

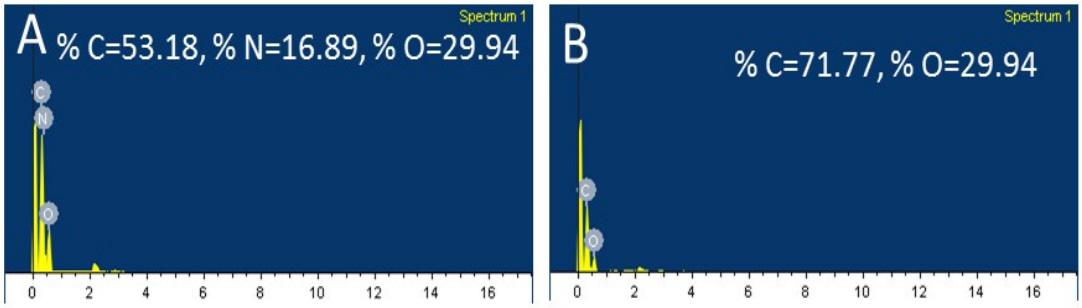

Fig. S1 EDAX profiles of pristine (A) SF; and (B) SFC showing increase in carbon content in coated sample.

2. TGA Analysis

   TGA analysis provided an insight into the thermal stability of SF after deposition of CNPs. It was observed that the SF and SFC are thermally stable upto 250 ^{o}C but degradation starts at 260 ^{o}C for SF and 284 ^{o}C for SFC while complete degradation was observed at 600 ^{o}C. The enhancement of thermal stability of SFC can assigned to reinforcement of SF with CNTs. The thermogram corresponding to SF and SFC is provided in **Fig. S2.**

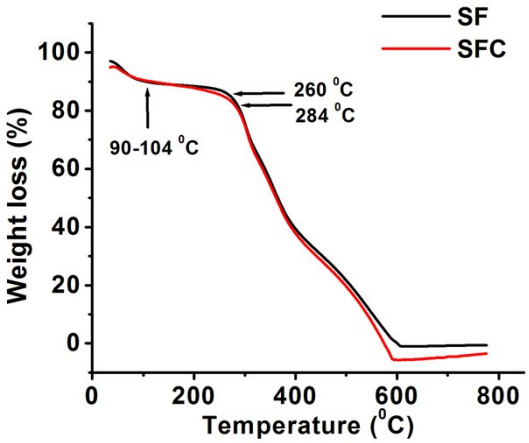

Fig. S2 TGA of SF and SFC

3. **%Z vs. conc. of explosive vapors (TNP/TNT)**

   The variation of % Z with concentrations of TNP and TNT vapors are depicted in **Fig. S3.**

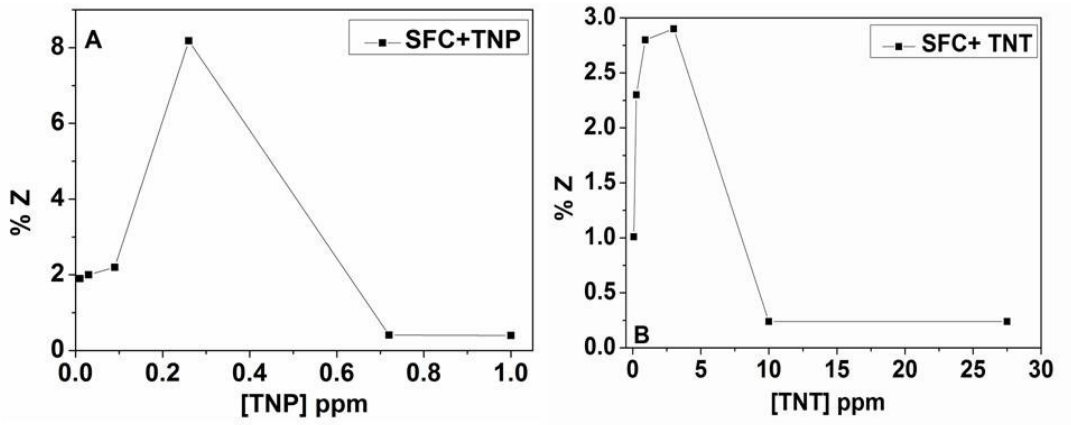

Fig. S3 Variation of % Z of SFC with (A)TNP and (B) TNT.

4. **Time interval measurement of SFC with TNP and TNT at different frequencies**

   The variation of log (Z) of SFCP and SFCT at 100 Hz, 10 KHz and 100 KHz are depicted below in **Fig. S4.**

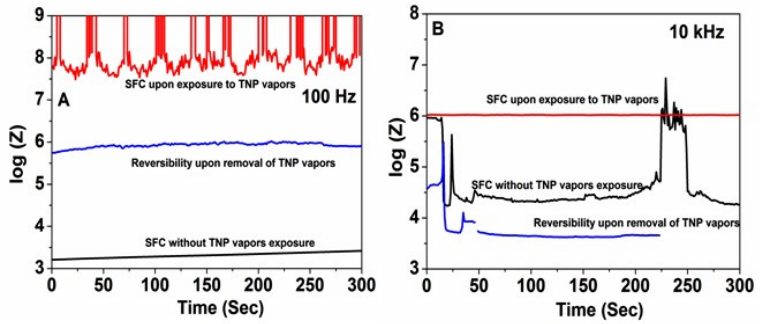

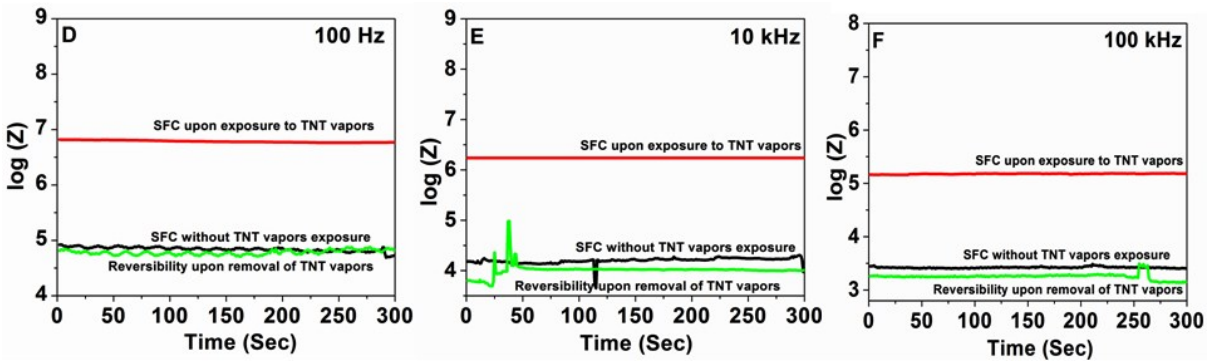

Fig. S4. Time interval measurements of SFC with TNP and TNT vapors at 100 Hz, 10 kHz and 100 kHz.

5. **I-V measurement of SF and SFC**

The conductivity switching behavior of SF and SFC are studied in detail. The conductivity change upon coating with CNPs on SF was observed from I-V plot given below in **Fig. S5.**

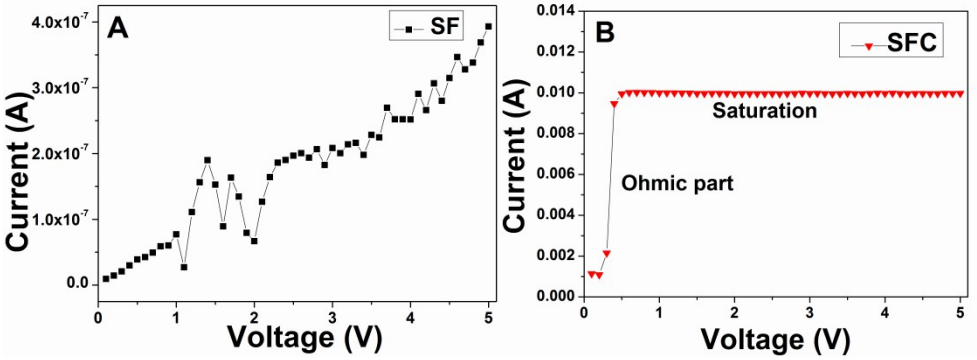

Fig. S5 I-V plot of A. SF and B. SFC

6. **Comparative FT-IR of SFC, SFCP and SFCT**

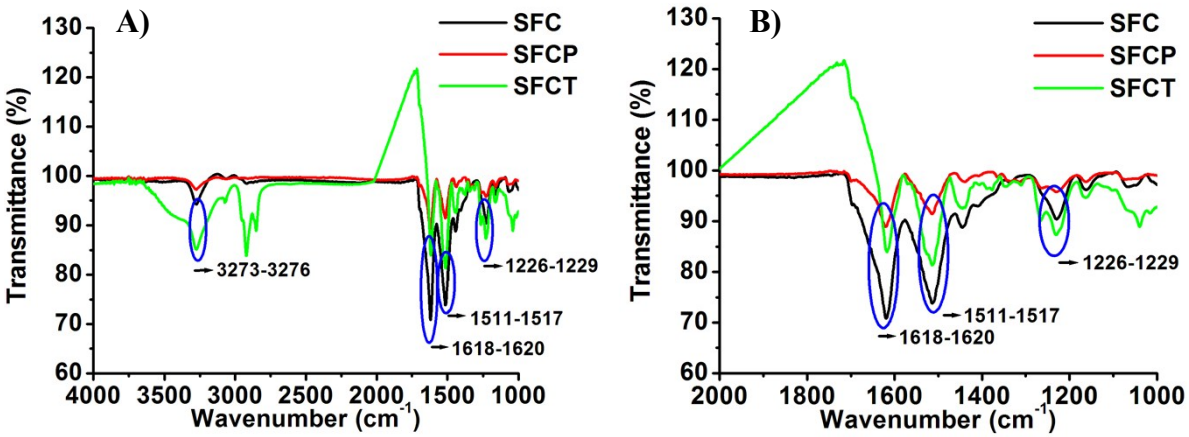

Fig. S6. FT-IR spectra showing stretching frequencies of SFC, SFCP and SFCT (A) and narrow range (B).

7. **TGA plots of SFC, SFCP and SFCT**

Thermograms showing thermal stabilities of SFC, SFCP and SFCT (**Fig. S7**).

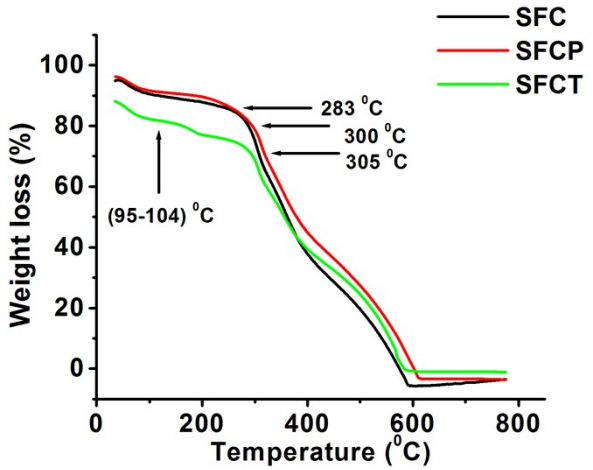

Fig. S7 Thermograms showing thermal stabilities of SFC, SFCP and SFCT

8. **Selectivity**

The selectivity studies were carried for 2-Nitrophenol (2NP), 4-Nitrophenol (4NP), 1, 4-Dinitrobenzene (DNB), 1,3- dinitrosalicylic acid (DNSA) and Benzene (**Fig. S8**.). The sensor was found to be effective for aromatic compounds bearing nitro functionalities.

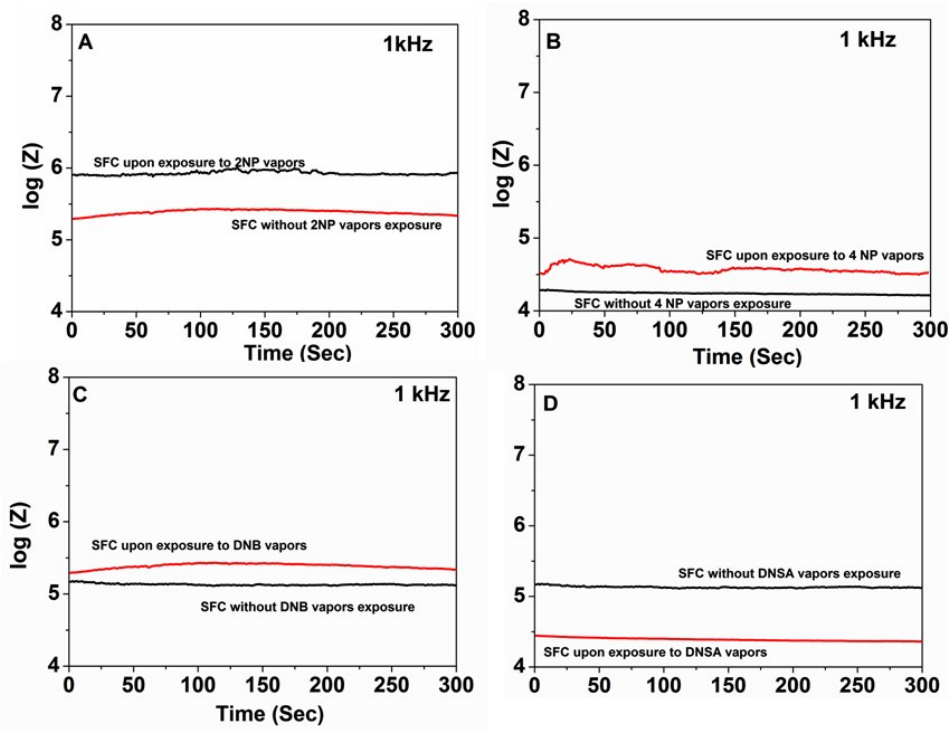

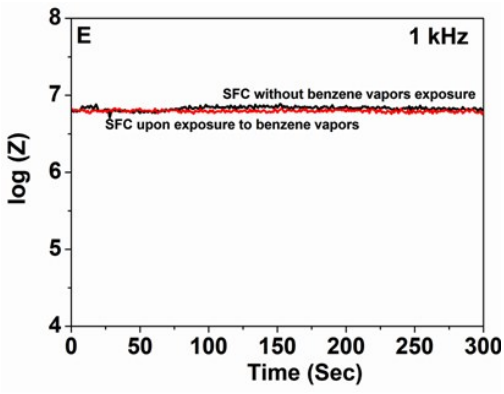

Fig. S8 Time interval measurements at 1 kHz of SFC with vapors of (A) 2NP; (B) 4NP; (C) DNB; (D) DNSA and (E) Benzene.

9. **Calibration curve**

The calibration curves were constructed for SFCP and SFCT for the calculation of limit of detection (LOD) which were found to be 0.39 ppm for TNP and 4.62 ppm for TNT respectively (**Fig. S9**).

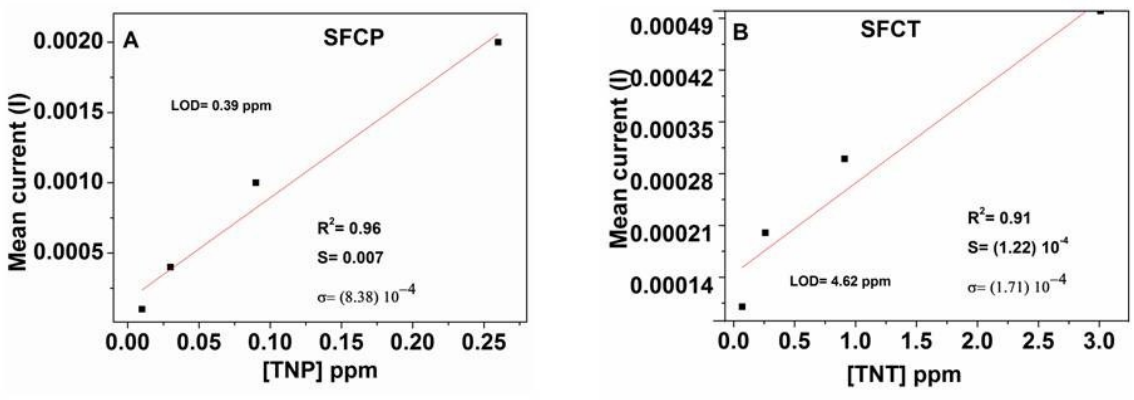

Fig. S9 Calibration curves for (A) SFCP and (B) SFCT